Published in final edited form as:
Eur J Neurosci. 2009 March ; 29(6): 1119–1130. doi:10.1111/j.1460-9568.2009.06664.x.

Neuroprotective activities of activated protein C mutant with reduced anticoagulant activity

Huang Guo[1,*], **Itender Singh**[1,*], **Yaoming Wang**[1,*], **Rashid Deane**[1], **Theresa Barrett**[1], **José A. Fernández**[2], **Nienwen Chow**[3], **John H. Griffin**[2], and **Berislav V. Zlokovic**[1]

1*Departments for Neurosurgery and Neurology, Center for Neurodegenerative and Vascular Brain Disorders, University of Rochester Medical Center, 601 Elmwood Avenue, Box 670, Rochester, NY 14642, USA*

2*Department of Molecular and Experimental Medicine, The Scripps Research Institute, La Jolla, CA, USA*

3*ZZ Biotech Research Laboratory, Rochester, NY, USA*

Abstract

The anticoagulant activated protein C (APC) protects neurons and endothelium via protease activated receptor (PAR)1, PAR3 and endothelial protein C receptor. APC is neuroprotective in stroke models. Bleeding complications may limit the pharmacologic utility of APC. Here, we compared the 3K3A-APC mutant with 80% reduced anticoagulant activity and wild-type (wt)-APC. Murine 3K3A-APC compared with wt-APC protected mouse cortical neurons from *N*-methyl-D-aspartate-induced apoptosis with twofold greater efficacy and more potently reduced *N*-methyl-D-aspartate excitotoxic lesions *in vivo*. Human 3K3A-APC protected human brain endothelial cells (BECs) from oxygen glucose deprivation with 1.7-fold greater efficacy than wt-APC. 3K3A-APC neuronal protection required PAR1 and PAR3, as shown by using PAR-specific blocking antibodies and PAR1- and PAR3-deficient cells and mice. BEC protection required endothelial protein C receptor and PAR1. In neurons and BECs, 3K3A-APC blocked caspase-9 and -3 activation and induction of p53, and decreased the Bax/Bcl-2 pro-apoptotic ratio. After distal middle cerebral artery occlusion (dMCAO) in mice, murine 3K3A-APC compared with vehicle given 4:00 h after dMCAO improved the functional outcome and reduced the infarction volume by 50% within 3 days. 3K3A-APC compared with wt-APC multi-dosing therapy at 12:00 h, 1, 3, 5 and 7 days after dMCAO significantly improved functional recovery and reduced the infarction volume by 75% and 38%, respectively, within 7 days. The wt-APC, but not 3K3A-APC, significantly increased the risk of intracerebral bleeding as indicated by a 50% increase in hemoglobin levels in the ischemic hemisphere. Thus, 3K3A-APC offers a new approach for safer and more efficacious treatments of neurodegenerative disorders and stroke with APC.

Keywords

endothelial injury; endothelial protein C receptor; neuronal injury; permanent ischemic injury; protease activated receptor; protein C mutant

Correspondence: Dr Berislav V. Zlokovic, as above. E-mail: E-mail: berislav_zlokovic@urmc.rochester.edu.

*H.G., I.S. and Y.W. contributed equally to this work.

Introduction

Activated protein C (APC) is a serine protease with systemic anticoagulant activity and direct cellular effects that are mediated by the protein C (PC) cellular pathway (Mosnier *et al.*, 2007). The anticoagulant action of APC is mediated by the irreversible proteolytic inactivation of the coagulation factors Va and VIIIa with contributions from various cofactors. Independent of its anticoagulant activity, APC exerts direct cytoprotective effects resulting in: (i) cytoprotective alteration of gene expression profiles; (ii) anti-inflammatory activities; (iii) antiapoptotic activity; and (iv) protection of endothelial barriers (Joyce *et al.*, 2001; Riewald *et al.*, 2002; Cheng *et al.*, 2003; Domotor *et al.*, 2003; Mosnier and Griffin, 2003 Feistritzer and Riewald, 2005; Finigan *et al.*, 2005). The cytoprotective actions of APC are generally mediated by the G-protein-coupled receptor, protease activated receptor (PAR)1 (Mosnier *et al.*, 2007).

In the central nervous system, APC protects neurons and brain endothelial cells (BECs) from divergent types of injury by inhibiting both the intrinsic and extrinsic apoptotic pathways (Cheng *et al.*, 2003; Liu *et al.*, 2004; Cheng *et al.*, 2006; Guo *et al.*, 2004). PAR1 and PAR3 (Guo *et al.*, 2004), and endothelial PC receptor (EPCR) and PAR1 (Cheng *et al.*, 2003) are required for direct neuronal protection and for protection of brain endothelium, respectively by APC. Early post-ischemic application of APC is neuroprotective in rodent models of transient brain ischemia (Shibata *et al.*, 2001; Cheng *et al.*, 2003, 2006) and embolic stroke (Zlokovic *et al.*, 2005). More recent studies suggest that the neuroprotection of APC after transient ischemia could be extended up to 24:00 h (Thiyagarajan *et al.*, 2008). In murine injury models, APC protects against diabetic endothelial and glomerular injury (Isermann *et al.*, 2007) and multiple sclerosis (Han *et al.*, 2008) as well as against ischemia reperfusion injury in kidney and lung (see review, Mosnier *et al.*, 2007). APC has been approved by the U.S. Food and Drug Administration for use in adult severe sepsis (Bernard *et al.*, 2001) and is currently in Phase I/IIa clinical trials for ischemic stroke [The Activated Protein C in Acute Stroke Trial (APCAST); http://clinicaltrials.gov/ct2/show/NCT00533546?term=apc&rank=25].

Although APC has the potential to treat various neurodegenerative disorders, its anticoagulant activity poses a potential complication as it may increase the risk of bleeding. To construct APC variants with a reduced risk of bleeding, we altered factor Va binding sites in APC without affecting sites that recognize EPCR or PAR1 (Gale *et al.*, 2002). The anticoagulant action of APC primarily involves a cleavage site at Arg506 in factor Va, and the association of APC with factor Va for this cleavage primarily depends on positively charged residues in surface loops on the protease domain of APC, including loop 37 (residues 190–193), the Ca^{2+}-binding loop (residues 225–235) and the autolysis loop (residues 301–316). Here, we tested the neuroprotective activities of an APC mutant generated with three alanine mutations in the 37 loop (KKK191-193AAA), designated 3K3A-APC. The 3K3A-APC mutant has reduced anticoagulant activity (by about 80%) (Gale *et al.*, 2002) but retains normal antiapoptotic activity on immortalized human umbilical vein cells that required PAR1 and EPCR (Mosnier *et al.*, 2004). The present study shows that 3K3A-APC exerts potent neuroprotective actions that are superior to wild-type (wt)-APC and suggests that this APC mutant offers potential advantages for neuroprotective therapies.

Materials and methods

Reagents

Activated protein C preparations—Murine recombinant wt-APC, murine 3K3A-APC (KKK191-193AAA) and enzymatically inactive murine Ser360Ala-APC (S360A-APC) were prepared essentially as described previously (Gale *et al.*, 2002; Mosnier *et al.*, 2004). Human

wt-PC and 3K3A-PC stable cell lines were generated in Chinese hamster ovary (CHO) cells. The cells were grown in suspension in CD OptiCHO medium (Invitrogen, Carlsbad, CA, USA) containing 2 m_M $CaCl_2$, 10 μg/mL vitamin K and 2 m_M GlutaMAX (Invitrogen) in a 2 L Biowave bioreactor for production. A four-step purification procedure was used: capturing PC using FFQ resin (GE Healthcare, Piscataway, NJ, USA), purification of PC using an Uno Q column (Bio-Rad, Richmond, CA, USA), activation with recombinant human thrombin (ZymoGenetics, Seattle, WA, USA) and removal of thrombin using an Uno Q column. The purity of 3K3A-APC and wt-APC was determined by reduced sodium dodecyl sulfate-polyacrylamide gel electrophoresis/silver staining. There was no detectable thrombin in the purified APC preparations based on thrombin time clotting assays using purified fibrinogen.

Before use, the enzymatic activity of each APC preparation was determined by amidolytic assay and the concentration by enzyme-linked immunosorbent assay and/or A280 spectral analysis. In addition, an activated partial thromboplastin time clotting assay was used to determine the clotting times of wt-APC and 3K3A-APC. A fresh aliquot of APC sample was used each time on the day of experiment.

Protease activated receptor-specific antibodies—All antibodies against PARs were from Santa Cruz Biotechnology (Santa Cruz, CA, USA). We used the following cleavage-site-blocking PAR antibodies: polyclonal rabbit against human PAR1 (H-111), monoclonal mouse against human PAR2 (SAM-11), polyclonal rabbit against human PAR3 (H-103) and polyclonal goat against mouse PAR4 (S-20). As control antibodies we used polyclonal goat against mouse PAR1 N-terminus (S-19), polyclonal goat against mouse PAR2 N-terminus (S-19), polyclonal goat against mouse PAR3 C-terminus (M-20) and polyclonal goat against mouse PAR4 C-terminus (M-20). As reported, these antibodies cross-react with the corresponding mouse and human PARs (Riewald *et al.*, 2002; Guo *et al.*, 2004).

Below are citations of publications for each of the key anti-PAR antibodies that have been shown to block activation of the respective PARs.

The H-111 anti-PAR1 antibody (polyclonal anti-PAR1 residues 1–111) was used to block the action of thrombin on PAR1 (Neaud *et al.*, 2004), as well as in several publications from our own laboratory (e.g. Cheng *et al.*, 2003; Guo *et al.*, 2004).

The SAM-11 anti-PAR2 antibody (anti-PAR2 residues 37–50, cleavage site) is a monoclonal antibody against a small peptide epitope comprising the activation cleavage site sequence in PAR2, and it has been used in peer-reviewed papers to either detect PAR2 or to block PAR2 activation. The failure of this antibody to appreciably block the actions of APC is excellent evidence that PAR2 activation does not play a significant role in the actions of APC. For previous validation of this monoclonal antibody, see for example: Dai *et al.* (2007), Kelso *et al.* (2007), Olianas *et al.* (2007) and Csernok *et al.* (2006).

The H-103 anti-PAR3 antibody (polyclonal anti-residues 1–103) has been used in multiple peer-reviewed papers (see for example Uehara *et al.*, 2003; Kim *et al.*, 2004; Pompili *et al.*, 2004).

The S-20 anti-PAR4 antibody (polyclonal anti-N terminal region) has been used in peer-reviewed papers (Balcaitis *et al.*, 2003; Pompili *et al.*, 2004; Yun *et al.*, 2007).

Other anti-PAR antibodies were used as negative controls to show that they had no ability to block the actions of APC; they have not been reported to block PAR activation for other known PAR agonist proteases.

Other reagents—*N*-methyl-D-aspartate (NMDA) was purchased from Sigma (St Louis, MO, USA). For western blot analysis the following antibodies were used: polyclonal rabbit antibody against human p53 (1 : 1000, Cell Signaling, Beverly, MA, USA), human Bcl-2 (1 : 1000, Cell Signaling) and human Bax (1 : 1000, Cell Signaling), which cross-react with the corresponding mouse proteins. The inhibitory peptides, Ac-DEVD-CHO (caspase-3, Sigma) and z-LEHD-fmk (caspase-9, Calbiochem, Gibbstown, NJ, USA), were selected on the basis of substrate specificity (Budd *et al.*, 2000). We used Hoechst 33342 (1 : 10 000; Molecular Probes, Eugene, OR, USA) for nucleic acid staining.

Mouse neuronal cell cultures

Pregnant mice were anesthetized with i.p. ketamine (100 mg/kg) and xylazine (10 mg/kg). All procedures were performed in accordance with protocols approved by the NIH and the Institutional Committee at the University of Rochester. Primary neuronal cultures were established as described previously (Bonfoco *et al.*, 1995; Guo *et al.*, 2004). In brief, cerebral cortex was dissected from fetal C57BL 6J mice (total of 40 pups), PAR1 null mice (total of 20 pups, on C57BL/6J background) (Connolly *et al.*, 1997) and PAR3 null mice (total of 18 pups, on C57BL/6J background) (Nakanishi-Matsui *et al*., 2000) at 16 days of gestation, treated with trypsin for 10 min at 37°C and dissociated by trituration. Dissociated cell suspensions were plated at 5×10^5 cells per well on 12-well tissue culture plates or at 4×10^6 cells per dish on 60 mm tissue culture dishes coated with poly-L-lysine, in serum-free Neurobasal medium plus B27 supplement (Gibco, Rockville, MA, USA). Cultures were maintained in a humidified 5% CO_2 incubator at 37°C for 7 days before treatment. The medium was replaced every 3 days.

It has been shown that differences in the number of contaminating astrocytes and in embryonic age at harvest contribute to the variability of cortical cultures (Romito-DiGiacomo *et al.*, 2007). In this study, we used embryonic day 16 mouse cortical cells cultured in Neurobasal medium with B27 supplement. Under these experimental conditions, glial growth could be reduced to <0.5% of the nearly pure neuronal population, as demonstrated by immnocytochemistry for glial fibrillary acidic protein (Brewer *et al.*, 1993). In our earlier studies (Guo *et al.*, 2004; Liu *et al.*, 2004) and in the present study, contamination of cortical neurons with astrocytes varied between 0.3% and 1%. If cerebral cortices were harvested at a somewhat later stage, i.e. embryonic day 17–18, or at an earlier stage at embryonic day 12, different proportions of astrocytes and/or the presence of neuronal progenitor cells were found. These preparations, however, were not used in the present experiments.

N-methyl-D-aspartate-induced apoptosis in neuronal culture

For induction of neuronal apoptosis, cultures were exposed for 10 min to 300 μM NMDA/5 μM glycine in Mg^{2+}-free Earle's balanced salt solution (Bonfoco *et al.*, 1995). Control cultures were exposed to Earle's balanced salt solution alone. After the exposure, cultures were rinsed with Earle's balanced salt solution, returned to the original culture medium and incubated with or without different concentrations of mouse recombinant wt-APC (2–20 nM), mouse 3K3A-APC (2–20 nM) and mouse S360A-APC (20 nM). All experiments involving treatment with APC included hirudin (1 μg/mL; Sigma) to block any thrombin signaling (Riewald *et al.*, 2002; Cheng *et al.*, 2003; Riewald and Ruf, 2005).

Intrastriatal N-methyl-D-aspartate microinjections in mice

We used an NMDA model of excitotoxic lesions in the mouse brain *in vivo*, as described previously (Ayata *et al.*, 1997; Guo *et al.*, 2004). All procedures were performed in accordance with protocols approved by the NIH and the Institutional Committee at the University of Rochester. Male C57BL6 mice (total of 20 mice), PAR1 null mice (total of 10 mice) (Connolly *et al*., 1997), PAR2 null mice (total of 10 mice) (Schmidlin *et al*., 2002) (Jackson Laboratory) and PAR3 null mice (total of 10 mice) (Nakanishi-Matsui *et al*., 2000) weighing 23–25 g were

used throughout the study. PAR1 null, PAR2 null and PAR3 null mice were on C57BL/6J background. Mice were anesthetized with i.p. ketamine (100 mg/kg) and xylazine (10 mg/kg) or with 1.5% isoflurane (in 70% nitric oxide and 30% oxygen). Animals received micro-infusions into the right striatum (0.5 mm anterior, 2.5 mm lateral, 3.2 mm ventral to the bregma) of either vehicle, NMDA (20 nmol in 0.3 μL of phosphate-buffered saline, pH 7.4), NMDA + murine wt-APC (0.2 μg), NMDA + murine 3K3A-APC (0.2 μg) or NMDA + murine 3K3A-APC (0.2 μg), + anti-PAR2 (SAM-11) or + anti-PAR4 (S-20) antibody (0.2 μg). The solutions were infused over 2 min using a micro-injection system (World Precision Instruments, Sarasota, FL, USA). The needle was left in place for an additional 8 min after the injection, as reported previously (Ayata *et al.*, 1997; Guo *et al.*, 2004). After 48:00 h mice were anesthetized intraperitoneally (i.p.) with a mixture of ketamine (100 mg/kg) and xylazine (10 mg/kg) and transcardially perfused with phosphate-buffered saline, pH 7.4, followed by 4% paraformaldehyde. The brains were removed and coronal sections of 30 μm thickness were prepared using a Vibratome. Every fifth section 1 mm anterior and posterior to the site of injection was stained with cresyl violet. The lesion area was identified by the loss of staining as reported previously (Ayata *et al.*, 1997; Guo *et al.*, 2004). The lesion areas were determined by an image analyser (Image-ProPlus, Media Cybernetics, Silver Spring, MD, USA) and integrated to obtain the volume of injury.

Human brain endothelial cell cultures

Primary BECs were isolated from cortical tissue after brain surgery for epilepsy. BECs were characterized and cultured, as we described elsewhere (Cheng *et al.*, 2006). Cells were maintained in serum-free Dulbecco's modified Eagle's medium and exposed for 1:00–8:00 h to oxygen/glucose deprivation (OGD) (<2% oxygen, no glucose). OGD was induced using an anaerobic chamber (Forma Scientific, Holbrook, New York, USA) (Cheng *et al.*, 2003). The levels of O_2 were monitored by O_2 Fyrite (Forma Scientific). Different concentrations of human recombinant wt-APC (3–100 n_M) and human recombinant 3K3A-APC (3–100 n_M) were added at the time of OGD treatment. Hirudin (1 μg/mL) was included to block any thrombin signaling (Riewald *et al.*, 2002; Cheng *et al.*, 2003; Riewald and Ruf, 2005).

Detection of apoptosis and cell injury

Apoptotic cells were visualized by *in-situ* terminal deoxynucleotidyl transferase-mediated digoxigenin-dUTP nick-end labeling assay according to the manufacturer's instructions (Promega, Madison, WI, USA). Cells were counterstained with the DNA-binding fluorescent dye Hoechst 33342 (Molecular Probes, Eugene, OR, USA) at 1 mg/mL for 10 min at room temperature (20°C) to reveal nuclear morphology. Cell survival of neurons was detected by using a 2-(2-methoxy-4-nitrophenyl)-3-(4-nitrophenyl)-5-(2,4-disulfophenyl)-2H-tetrazolium monosodium salt (WST-8) assay (Dojindo Molecular Technologies, Gaithersburg, ML, USA). The WST-8 assay determines the amount of water-soluble formazan product in contrast to the 3-(4,5-dimethylthiazol-2-yl)-5-(3-carboxymethaxyphenyl)-2-(4-sulfophenyl)- 2H-tetrozolium (MTT) assay, which determines the levels of water-insoluble formazan product (Isobe *et al.*, 1999). The amount of WST-8 (yellow color) is directly proportional to the number of living cells as it is produced by the activity of dehydrogenases in cells. Thus, the absorbance at 460 nm of WST formazan is directly proportional to the number of viable cells in the medium. Cell injury of human BECs exposed to hypoxia was detected by the release of lactate dehydrogenase (LDH) (LDH assay, Sigma), as reported previously (Cheng *et al.*, 2003).

Western blot analyses

Whole cellular extracts and nuclear protein fractions were prepared and the protein concentration determined using the Bradford protein assay (Bio-Rad, Hercules, CA, USA); 10–50 μg of protein was analysed by 10% sodium dodecyl sulfate-polyacrylamide gel

electrophoresis and transferred to nitrocellulose membranes that were then blocked with 5% non-fat milk in Tris-buffered saline (100 mM Tris, pH 8.0, 1.5 M NaCl, 0.1% Tween 20) for 1:00 h. The membranes were incubated overnight with primary antibodies, washed with Tris-buffered saline and incubated with a horseradish peroxidase-conjugated secondary antibody for 1:00 h. Immunoreactivity was detected by using the ECL detection system (Amersham, Piscataway, NJ, USA).

Caspase-3 and -9 activity

Cells were washed with phosphate-buffered saline and resuspended in cell lysis buffer; 50 μL of lysates was incubated with 50 μM caspase-3 (DEVD-pNA) or caspase-9 (Ac-LEHD-pNA) substrate at 37°C (ApoAlert caspase assay kit, Clontech, Palo Alto, CA, USA). Substrate hydrolysis was determined as the change in $A_{405\ nm}$ using a microplate reader and enzymatic activity was expressed in arbitrary units per mg of protein.

Permanent distal middle cerebral artery occlusion

All procedures were approved by the Institutional Animal Care and Use Committee at the University of Rochester. Male C57BL6 mice (total of 25 mice), 6–8 weeks old, were anesthetized with ketamine (100 mg/kg, i.p.) and xylazine (10 mg/kg, i.p.). The physiological parameters were monitored as described previously (Wang *et al.*, 1997). Briefly, animals were allowed to breathe spontaneously. Rectal temperature was maintained at 37 °C using a feedback-controlled heating system. The right femoral artery was cannulated for continuous monitoring of blood pressure and blood analysis including pO_2, pCO_2 and pH. Under the surgical microscope, the left common carotid artery was isolated through a neck incision and ligated using a 5-0 silk. A skin incision was made between the right orbit and tragus. The zygomatic arch was removed and temporal muscle retracted laterally. The mandible was retracted downward. The middle cerebral artery (MCA) was visible through the temporal semi-translucent surface of the skull. Craniectomy was performed by drilling with a 0.9 mm round burr. The inner layer of the skull was removed with fine forceps. The dura was carefully opened and the M1 branch of the MCA exposed and coagulated using a cauterizer, producing permanent distal MCA occlusion (dMCAO) (Zhang *et al.*, 2005). The wound was sutured and rectal temperature was controlled until mice regained full consciousness.

All studies were performed in a blind fashion. Mice were randomly assigned to the vehicle-treated group, murine wt-APC-treated group and murine 3K3A-APC-treated group. For the multi-dosing treatment, wt-APC and 3K3A-APC were administered intravenously by the tail vein at 0.2 mg/kg at 12:00 h, 1, 3, 5 and 7 days after dMCAO. The vehicle-treated group received saline. At days 1, 3 and 7 post-ischemia the functional recovery was assessed by the forelimb asymmetry test for sensory-motor activity and foot-fault test for locomotor assessment (Wang *et al.*, 2009). Mice were anesthetized i.p. with a mixture of ketamine (100 mg/kg) and xylazine (10 mg/kg) and killed by decapitation after 7 days and the brains removed and rapidly frozen in CO_2 snow. Brains were cut into serial 20 μm cryostat sections. Every 10th section was stained with cresyl violet for determination of the infarct volume using the NIH Image J analysis system.

Hemoglobin levels in the ischemic hemisphere were determined using a spectrophotometric hemoglobin assay, as described previously (Shibata *et al.*, 2001; Cheng *et al.*, 2006). Briefly after cresyl violet staining, the hemisections of the ischemic hemisphere were homogenized and treated with Darbkin reagent (Sigma) to determine hemoglobin content. Mouse blood added to brain homogenates was used for standard curves.

For the single dose treatment, 3K3A-APC (0.2 mg/kg) or saline was administered by the tail vein at 4:00 h after dMCAO. At days 1 and 3 post-ischemia, the forelimb asymmetry test and

foot-fault test were performed. The mice were anesthetized i.p. with a mixture of ketamine (100 mg/kg) and xylazine (10 mg/kg) and killed by decapitation after 3 days and the brains processed for the infarct volume measurements as described above.

Statistical analysis

Data are presented as mean ± SEM. Student's *t*-test and one- or two-way ANOVA followed by a post-hoc Tukey test were used to determine statistically significant differences. The curves of functional recovery after stroke were compared using repeated-measures ANOVA. $P < 0.05$ was considered statistically significant.

Results

Recombinant murine 3K3A-APC reduced the number of NMDA-treated terminal deoxynucleotidyl transferase-mediated digoxigenin-dUTP nick-end labeling-positive mouse cortical neurons (Fig. 1a) and dose-dependently increased their cell survival (two-way ANOVA to compare 3K3A-APC vs. wt-APC concentration curves; a total of seven different concentrations of 3K3A-APC and wt-APC were used; $n = 5$ independent cultures per single concentration point for either 3K3A-APC or wt-APC, $P < 0.01$; Fig. 1b). The rate of spontaneous apoptosis in the culture medium in the absence of NMDA was low under the present experimental conditions, as shown by the cell survival of >90% (Fig. 1b, Vehicle). These findings are consistent with previous reports using similar culture media and experimental conditions (Tenneti and Lipton, 2000;Guo *et al.*, 2004). The survival rate of neurons challenged by NMDA alone was <40% (Fig. 1b, zero APC concentration on the abscissa), suggesting that >60% of neurons die within 24:00 h of exposure to NMDA. 3K3A-APC exhibited a higher neuroprotective efficacy than wt-APC (Fig. 1b) as also confirmed by their respective IC_{50} values of 3.03 ± 0.32 and 5.94 ± 0.54 n_M (Student's *t*-test, $P < 0.05$; values obtained from 35 independent cultures for either 3K3A-APC or wt-APC from Fig. 1b were taken for analysis; Fig. 1c). Hirudin alone did not have an effect on the survival of cortical neurons, i.e. survival with hirudin was 94.0 ± 4.5% (mean ± SEM, $n = 3$), similar to that of vehicle-treated controls.

The NMDA treatment of neurons compared with vehicle increased both caspase-9 and -3 activities (one-way ANOVA followed by Tukey's post-hoc test, $P < 0.05$; $n = 5$ independent cultures per treatment; Fig. 2a and b), as reported previously in several studies using similar concentrations of NMDA and exposure times as in the present study (Du *et al.*, 1997; Budd *et al.*, 2000; Tenneti and Lipton, 2000; Okamoto *et al.*, 2002; Guo *et al.*, 2004). It has been reported that different amplitudes and durations of NMDA signaling (e.g. 500 μ_M NMDA for 5 min (Wang *et al.*, 2004) compared with 300 μ_M NMDA for 10 min as in the present study and studies listed above) may elicit caspase-independent, poly (ADP-ribose) polymerase-1-mediated cell death, suggesting that the differences in the experimental conditions dictate the involvement of the prevailing apoptotic cascade in neurons challenged by NMDA. Generation of caspase-9 activity was almost completely inhibited by z-LEHD-fmk (caspase-9-specific inhibitor) as well as by 3K3A-APC and wt-APC but not by enzymatically inactive S360A-APC (Fig. 2a). Caspase-3 activity was completely inhibited by Ac-DEVD-CHO (caspase-3 specific inhibitor) (Fig. 2b) and by z-LEHD-fmk, suggesting that caspase-9 activity is upstream to caspase-3 activation in the present model, as reported previously (Guo *et al.*, 2004). Both 3K3A-APC and wt-APC, but not S360A-APC, inhibited the appearance of caspase-3 activity (Fig. 2b). Interestingly, the 3K3A-APC inhibition of both caspases was significantly higher than that observed for wt-APC at an equimolar concentration.

3K3A-APC suppressed p53 expression and decreased favorably the Bax : Bcl-2 pro-apoptotic ratio (Fig. 2c and d) (Student's *t*-test, $P < 0.05$; $n = 3$ independent blots per group; Fig. 2d). Increased p53 expression and an elevated pro-apoptotic Bax : Bcl-2 ratio have been described

previously in neurons after NMDA challenge (Uberti *et al.*, 1998; Djebaili *et al.*, 2000; Jordan *et al.*, 2003; Guo *et al.*, 2004). By reducing the Bax : Bcl-2 ratio, 3K3A-APC reduces the release of cytochrome *c* by stabilizing the permeability of the mitochondrial membrane, which blocks activation of caspases (Penninger and Kroemer, 2003).

By using specific cleavage-site-blocking PAR antibodies that block the action of the respective PARs and control N-terminus and C-terminus PAR antibodies, we obtained data implying that PAR1 and PAR3 are required for 3K3A-APC-mediated neuronal protection against NMDA injury (one-way ANOVA followed by Tukey's post-hoc test, $P < 0.01$; $n = 3$ independent cultures per treatment; Fig. 3a). Please see Materials and methods for citations of publications for each of the key anti-PAR antibodies that were used in this experiment and have been shown to block activation of the respective PARs, which is the crucial point for showing specificity of the actions of wt or 3K3A-APC. This result was confirmed by demonstrating the loss of 3K3A-APC protection in cortical neurons derived from $PAR1^{-/-}$ and $PAR3^{-/-}$ mice compared with their respective controls (one-way ANOVA followed by Tukey's post-hoc test, $P < 0.01$; $n = 3$ independent cultures per treatment; Fig. 3b). It is of note that other PARs are expressed in PAR1 (Song *et al.*, 2005) and PAR3 (not shown) null mice.

We next studied whether the 3K3A-APC protection of cultured neurons against NMDA injury extends to an *in-vivo* model of NMDA-induced lesions in mouse brain (Ayata *et al.*, 1997). In these studies, murine 3K3A-APC compared with vehicle-treated controls significantly reduced NMDA-induced lesions within 48:00 h of intracerebral injections (Fig. 4a). The protective effect of the APC mutant was more pronounced than the protection observed with wt-APC at the same concentration (one-way ANOVA followed by Tukey's post-hoc test, $P < 0.05$; $n = 5$ mice per group; Fig. 4b). It is of note that the NMDA lesion volumes in control mice anesthetized with ketamine and xylazine compared with isoflurane were 5.43 ± 0.37 and 5.58 ± 0.51 mm^3, respectively ($n = 5$ mice per group; Fig. 4b, white and black bars, respectively). Thus, a brief systemic exposure to ketamine during an initial NMDA intracerebral administration did not have an effect on the spread of the NMDA lesion over the following 48:00 h, as reported by Guo *et al.* (2004), in spite of the fact that ketamine is an NMDA antagonist.

As *in vitro*, 3K3A-APC required *in vivo* the PAR1 and PAR3 receptors as demonstrated by using $PAR1^{-/-}$, $PAR2^{-/-}$ and $PAR3^{-/-}$ mice and catalytic-site-blocking PAR2 and PAR4 antibodies (one-way ANOVA followed by Tukey's post-hoc test, $P < 0.01$; $n = 5$ mice per group; Fig. 4c). Namely, 3K3A-APC did not protect against NMDA *in-vivo* toxicity in $PAR1^{-/-}$ and PAR3−/− mice compared with vehicle-treated controls but was fully effective in $PAR2^{-/-}$ mice (Fig. 4c), indicating that PAR1 and PAR3, but not PAR2, are critical for 3K3A-APC *in-vivo* protection. These results were additionally confirmed by demonstrating that 3K3A-APC protects in the presence of PAR2-blocking antibody (Fig. 4c). We also showed that the specific blockade of PAR4 action with PAR4-blocking antibody did not affect the 3K3A-APC-mediated reduction of the lesion volume, which was consistent with earlier data showing that wt-APC was neuroprotective in this model in $PAR4^{-/-}$ mice (Guo *et al.*, 2004). Future studies using PAR4 null mice should additionally confirm the present findings obtained in mice treated with 3K3A-APC- and PAR4-specific blocking antibodies by showing that PAR4 is not involved in the neuroprotection of 3K3A-APC.

It has been reported that, in the present NMDA *in-vivo* lesion model, PAR1 null and PAR3 null mice are not protected at the baseline (Guo *et al.*, 2004). This finding was confirmed and extended in the present study by showing no significant difference in the lesion volume in control mice (Fig. 4b) and $PAR1^{-/-}$ $PAR2^{-/-}$ and $PAR3^{-/-}$ mice (Fig. 4c), all on C57BL6 background and treated with vehicle. It is of note that the APC and NMDA distribution in the

brain after intracerebral injection is governed by the interstitial fluid bulk flow independent of their respective molecular weights (Zlokovic, 2008).

To determine whether 3K3A-APC also protects brain vascular cells, we studied its effects in an OGD model using human BECs, as described previously (Cheng *et al.*, 2003, 2006). In these studies we used human recombinant wt-APC and 3K3A-APC. 3K3A-APC exhibited significant antiapoptotic activity as demonstrated by a substantial reduction in terminal deoxynucleotidyl transferase-mediated digoxigenin-dUTP nick-end labeling-positive BECs (Fig. 5a). There was a dose-dependent protection of OGD-treated BECs by both 3K3A-APC and wt-APC (two-way ANOVA to compare 3K3A-APC vs. wt-APC concentration curves, $P < 0.01$; a total of seven different concentrations were used for either 3K3A-APC or wt-APC; $n = 4$ independent cultures for a single concentration point for either 3K3A-APC or wt-APC; Fig. 5b). The basal rate of BEC death under normoxic conditions was about 25%, as reported previously (Cheng *et al.*, 2003). The basal rate of BEC death with hirudin alone was about 26.2 ± 2.6% (mean ± SEM, $n = 3$), which was similar to normoxic controls. 3K3A-APC was more potent than wt-APC in view of their respective IC_{50} values of 8.44 ± 1.11 and 14.45 ± 0.96 n_M (Student's *t*-test, $P < 0.05$; values from 28 independent cultures taken from Fig. 5b were used for analysis for either 3K3A-APC or wt-APC; Fig. 5c).

As seen above for the neuronal protection of APC, 3K3A-APC inhibited p53 expression, decreased favorably the Bax : Bcl-2 ratio (Fig. 6a and b) (one-way ANOVA followed by Tukey's post-hoc test, $P < 0.05$; $n = 4$ different blots per group; Fig. 6b) and blocked the activation of caspase-9 and -3 (one-way ANOVA followed by Tukey's post-hoc test, $P < 0.05$; $n = 5$ independent cultures per treatment; Fig. 6c and d); its effects were more pronounced than those obtained with wt-APC. That both EPCR and PAR1 were required for the protection of 3K3A-APC of hypoxic BECs was indicated by the loss of protection in the presence of an EPCR antibody that inhibits APC binding to EPCR (RCR-252) (Fukudome *et al.*, 1998) but not with a non-blocking control EPCR antibody (RCR-92), and by blockade of the protection of 3K3A-APC with antibodies that block PAR1 proteolytic activation but not with antibodies that block PAR2, PAR3 and PAR4 proteolytic activation or other control anti-PAR antibodies (one-way ANOVA followed by Tukey's post-hoc test, $P < 0.05$; $n = 4$ independent cultures per treatment; Fig. 6e).

In the next set of experiments we studied the neuroprotective activities of murine 3K3A-APC and murine wt-APC in a stroke model. Physiological parameters, including arterial blood pressure, blood gases and pH before surgery and at 1:00 h after surgery, were not different between the control group and groups treated with wt-APC and 3K3A-APC (data not shown). However, future studies should carefully determine the effects of 3K3A-APC on blood flow regulation and different neurological functions. In a first set of studies, 3K3A-APC (0.2 mg/kg) or vehicle was administered at 4:00 h after dMCAO and certain functional and neuropathological outcomes determined within 3 days of ischemia onset. The 3K3A-APC dose was chosen based on previous findings demonstrating maximal protection with intravenous murine recombinant wt-APC at 0.2 mg/kg in murine models of transient MCA occlusion (Cheng *et al.*, 2003, 2006) and embolic stroke (Zlokovic *et al.*, 2005). As expected, 3K3A-APC substantially improved the performance of mice on the foot-fault and forelimb asymmetry tests (repeated-measures ANOVA, $P < 0.01$ for 3K3A-APC compared with vehicle; $n = 5$ mice per group; Fig. 7a and b) and reduced the infarction volume by 50% (Student's *t*-test, $P < 0.01$; $n = 5$ mice per group; Fig. 7c). As murine wt-APC at a higher dose was neuroprotective after transient MCA occlusion in mice within 24:00 h of ischemia onset (Thiyagarajan *et al.*, 2008), we next compared the effects of multi-dosing therapies with intravenous wt-APC and 3K3A-APC at 0.2 mg/kg administered at 12:00 h, 1, 3, 5 and 7 days after dMCAO. Over periods of 7 days after ischemia onset, 3K3A-APC almost normalized the performance of mice on the foot-fault and forelimb asymmetry tests (repeated-measures ANOVA, $P < 0.01$ for 3K3A-APC

vs. wt-APC; $P < 0.01$ for 3K3A-APC vs. vehicle; $n = 5$ mice per group; Fig. 8a and b). The wt-APC also significantly improved functional recovery but its beneficial effects were mid-way between the values found in vehicle-treated controls and 3K3A-APC-treated mice. Moreover, 3K3A-APC reduced the infarction volume at 7 days after dMCAO by 75% compared with 38% found with wt-APC (Fig. 8c and d) (one-way ANOVA followed by Tukey's post-hoc test, $P < 0.01$; $n = 5$ mice per group; Fig. 8d). Multiple-dosing treatment with wt-APC beginning at 12:00 h after dMCAO increased the hemoglobin levels in the ischemic brain hemisphere within 7 days by about 50% compared with vehicle-treated controls (one-way ANOVA followed by Tukey's post-hoc test, $P < 0.01$; $n = 5$ mice per group; Fig. 8e). In contrast, there was no increase in hemoglobin brain levels after 3K3A-APC, suggesting that the mutant protein reduces the risk of APC for bleeding.

Discussion

This study shows that 3K3A-APC, an APC mutant with greatly reduced anticoagulant activity (Gale *et al.*, 2002; Mosnier *et al.*, 2004), fully retains its cytoprotective activities in NMDA models of neuronal injury *in vitro* and *in vivo*, protects human BECs from OGD-induced apoptosis and is neuroprotective in a stroke model. When compared with recombinant wt-APC, 3K3A-APC was more efficacious in all studied models of neuronal and brain endothelial injury *in vitro*, achieving a protection similar to that of wt-APC at doses that were about half of those of wt-APC. 3K3A-APC also provided greater neuroprotection than wt-APC *in vivo* in models of excitotoxic brain lesions and stroke, and reduced the risk of intracerebral bleeding.

The APC mutants with reduced anticoagulant activity but normal cytoprotective activities are as beneficial in animal models of sepsis as wt-APC (Kerschen *et al.*, 2007), while reducing the risk of bleeding due to reductions in the anticoagulant and profibrinolytic activities of APC (Mosnier *et al.*, 2007). Recombinant wt-APC or plasma-derived APC within a therapeutic range of concentrations as used in animal models of organ reperfusion injury, including lung, kidney and brain, or in models of thrombosis and sepsis, did not cause bleeding (Griffin *et al.*, 2002; Mosnier *et al.*, 2007). However, when applied at a higher pharmacological dose, a recombinant APC with an increased anticoagulant activity killed monkeys by producing disseminated bleeding in various organs (http://www.emea.europa.eu/humandocs/PDFs/EPAR/xigris/247102en6.pdf) and increased the risk of intracerebral bleeding in a stroke model (Wang *et al.*, 2009).

The successful PROWESS (The Recombinant Human Activated Protein C Worldwide Evaluation in Severe Sepsis) trial for APC infusions in adult patients with severe sepsis was also associated with a low but significant risk of bleeding including cerebral hemorrhage (Bernard *et al.*, 2001).

In addition to ischemic stroke, APC has demonstrated beneficial effects in animal models of spinal cord injury (Taoka *et al.*, 2000), amyotrophic lateral sclerosis (Zhong *et al.*, 2006) and multiple sclerosis (Han *et al.*, 2008), and reduced tissue plasminogen activator-mediated neurotoxicity *in vivo* (Cheng *et al.*, 2003, 2006). Although the inflammatory reactions might be different after ischemia/reperfusion, based on previous work with wt-APC demonstrating its effectiveness in ischemia reperfusion models (Shibata *et al.*, 2001; Cheng *et al.*, 2003, 2006), one might expect that 3K3A-APC will also be effective after transient brain ischemia as it is after permanent ischemia. It has been recently reported that wt-APC and its analogs with reduced anticoagulant activity including 3K3A-APC cross the intact blood-brain barrier via EPCR-mediated transport (Deane *et al.*, 2008). Therefore it is possible that the direct action of 3K3A-APC on neurons contributes to the observed neuroprotection *in vivo*. A greater benefit to the neurological function after daily administration than after a single dose of 3K3A-APC suggests that the mutant protein can prevent progression of the ischemic injury.

The three alanine mutations in a factor Va binding site on the protease domain of 3K3A-APC do not affect the N-terminal Gla domain of APC, which binds to EPCR on the surface of endothelial cells, and do not alter the proteolytic active site mediating the activation of PAR1 (Mosnier *et al.*, 2007). The present findings are consistent with several earlier reports that did not show PAR3 involvement in APC-mediated effects on systemic endothelial cells and/or BECs (Cheng *et al.*, 2003; Feistritzer and Riewald, 2005; Finigan *et al.*, 2005; Riewald and Ruf, 2005). These studies and the present data support the view that APC and its non-anticoagulant 3K3A-APC mutant require PAR1 and EPCR for their direct effects on endothelium. However, 3K3A-APC required both PAR1 and PAR3 for its actions on neurons, similar to wt-APC (Guo *et al.*, 2004).

The observed greater efficacy of 3K3A-APC compared with wt-APC in models of neuronal and BEC injury must be derived from structural differences between the mutant protein and wt-APC and their different abilities to interact with PAR1 and/or other putative APC receptors. These may include, in addition to a different amino acid composition in loop 37, different post-translational modifications of the mutant protein compared with wt-APC during processing, resulting in different contents of negatively charged sialic acid and/or different distribution and branching of the N-linked glycan species. The exact biochemical mechanisms for the mutant enhanced efficacy compared with wt-APC remain, however, to be explored by future studies that should determine the temporal pattern and dose-dependency of PAR1 activation, interaction with other APC receptors, such as sphingosine-1-phosphate, EPCR or PAR3 (Guo *et al.*, 2004; Feistritzer and Riewald, 2005; Finigan *et al.*, 2005), and the magnitude and temporal profile of activation of the antiapoptotic pathways by the two proteins.

In summary, our findings suggest that 3K3A-APC may offer a new approach for more efficacious treatments of stroke and other neurodegenerative disorders that are based on APC therapies.

Acknowledgements

This work was supported by the National Institutes of Health grants HL63290 and HL81528 (B.V.Z.). We thank Dayle Schweibert for producing recombinant human 3K3A-APC in the bioreactor, Michael Sperber for purifying the protein and Sarah Lawrence for the initial characterization of 3K3A-APC. We also thank Dr Xin Tu (Department of Biostatistics and Computational Biology at the University of Rochester) for his assistance with statistical analysis.

Abbreviations

APC, activated protein C
BEC, brain endothelial cell
CHO, Chinese hamster ovary
dMCAO, distal middle cerebral artery occlusion
EPCR, endothelial protein C receptor
LDH, lactate dehydrogenase
MCA, middle cerebral artery
MTT, 3-(4,5-dimethylthiazol-2-yl)-5-(3-carboxymethoxyphenyl)-2-(4-sulfophenyl)-2H-tetrazolium
NMDA, *N*-methyl-D-aspartate
OGD, oxygen / glucose deprivation
PAR, protease activated receptor
PC, protein C
WST-8, 2-(2-methoxy-4-nitrophenyl)-3-(4-nitrophenyl)-5-(2,4-disulfophenyl)-2H-tetrazolium monosodium salt; wt, wild-type.

References

Ayata C, Ayata G, Hara H, Matthews RT, Beal MF, Ferrante RJ, Endres M, Kim A, Christie RH, Waeber C, Huang PL, Hyman BT, Moskowitz MA. Mechanisms of reduced striatal NMDA excitotoxicity in type I nitric oxide synthase knock-out mice. J. Neurosci 1997;17:6908–6917. [PubMed: 9278526]

Balcaitis S, Xie Y, Weinstein JR, Andersen H, Hanisch UK, Ransom BR, Moller T. Expression of proteinase-activated receptors in mouse microglial cells. Neuroreport 2003;14:2373–2377. [PubMed: 14663194]

Bernard GR, Vincent JL, Laterre PF, LaRosa SP, Dhainaut JF, Lopez-Rodriguez A, Steingrub JS, Garber GE, Helterbrand JD, Ely EW, Fisher CJ Jr. Efficacy and safety of recombinant human activated protein C for severe sepsis. N. Engl. J. Med 2001;344:699–709. [PubMed: 11236773]

Bonfoco E, Krainc D, Ankarcrona M, Nicotera P, Lipton SA. Apoptosis and necrosis: two distinct events induced, respectively, by mild and intense insults with N-methyl-D-aspartate or nitric oxide/superoxide in cortical cell cultures. Proc. Natl. Acad. Sci. U S A 1995;92:7162–7166. [PubMed: 7638161]

Brewer GJ, Torricelli JR, Evege EK, Price PJ. Optimized survival of hippocampal neurons in B27-supplemented Neurobasal, a new serum-free medium combination. J. Neurosci. Res 1993;35:567–576. [PubMed: 8377226]

Budd SL, Tenneti L, Lishnak T, Lipton SA. Mitochondrial and extramitochondrial apoptotic signaling pathways in cerebrocortical neurons. Proc. Natl. Acad. Sci. U S A 2000;97:6161–6166. [PubMed: 10811898]

Cheng T, Liu D, Griffin JH, Fernandez JA, Castellino F, Rosen ED, Fukudome K, Zlokovic BV. Activated protein C blocks p53- mediated apoptosis in ischemic human brain endothelium and is neuroprotective. Nat. Med 2003;9:338–342. [PubMed: 12563316]

Cheng T, Petraglia AL, Li Z, Thiyagarajan M, Zhong Z, Wu Z, Liu D, Maggirwar SB, Deane R, Fernandez JA, LaRue B, Griffin JH, Chopp M, Zlokovic BV. Activated protein C inhibits tissue plasminogen activator-induced brain hemorrhage. Nat. Med 2006;12:1278–1285. [PubMed: 17072311]

Connolly AJ, Suh DY, Hunt TK, Coughlin SR. Mice lacking the thrombin receptor, PAR1, have normal skin wound healing. Am. J. Pathol 1997;151:1199–1204. [PubMed: 9358744]

Csernok E, Ai M, Gross WL, Wicklein D, Petersen A, Lindner B, Lamprecht P, Holle JU, Hellmich B. Wegener autoantigen induces maturation of dendritic cells and licenses them for Th1 priming via the protease-activated receptor-2 pathway. Blood 2006;107:4440–4448. [PubMed: 16478888]

Dai Y, Wang S, Tominaga M, Yamamoto S, Fukuoka T, Higashi T, Kobayashi K, Obata K, Yamanaka H, Noguchi K. Sensitization of TRPA1 by PAR2 contributes to the sensation of inflammatory pain. J. Clin. Invest 2007;117:1979–1987. [PubMed: 17571167]

Deane R, Larue B, Sagare AP, Castellino FJ, Zhong Z, Zlokovic BV. Endothelial protein C receptor-assisted transport of activated protein C across the mouse blood-brain barrier. J. Cereb. Blood Flow Metab. 2008

Djebaili M, Rondouin G, Baille V, Bockaert J. p53 and Bax implication in NMDA induced-apoptosis in mouse hippocampus. Neuroreport 2000;11:2973–2976. [PubMed: 11006977]

Domotor E, Benzakour O, Griffin JH, Yule D, Fukudome K, Zlokovic BV. Activated protein C alters cytosolic calcium flux in human brain endothelium via binding to endothelial protein C receptor and activation of protease activated receptor-1. Blood 2003;101:4797–4801. [PubMed: 12586611]

Du Y, Bales KR, Dodel RC, Hamilton-Byrd E, Horn JW, Czilli DL, Simmons LK, Ni B, Paul SM. Activation of a caspase 3-related cysteine protease is required for glutamate-mediated apoptosis of cultured cerebellar granule neurons. Proc. Natl. Acad. Sci. U S A 1997;94:11657–11662. [PubMed: 9326666]

Feistritzer C, Riewald M. Endothelial barrier protection by activated protein C through PAR1-dependent sphingosine 1-phosphate receptor-1 crossactivation. Blood 2005;105:3178–3184. [PubMed: 15626732]

Finigan JH, Dudek SM, Singleton PA, Chiang ET, Jacobson JR, Camp SM, Ye SQ, Garcia JG. Activated protein C mediates novel lung endothelial barrier enhancement: role of sphingosine 1-phosphate receptor transactivation. J. Biol. Chem 2005;280:17286–17293. [PubMed: 15710622]

Fukudome K, Ye X, Tsuneyoshi N, Tokunaga O, Sugawara K, Mizokami H, Kimoto M. Activation mechanism of anticoagulant protein C in large blood vessels involving the endothelial cell protein C receptor. J. Exp. Med 1998;187:1029–1035. [PubMed: 9529319]

Gale AJ, Tsavaler A, Griffin JH. Molecular characterization of an extended binding site for coagulation factor Va in the positive exosite of activated protein C. J. Biol. Chem 2002;277:28836–28840. [PubMed: 12063259]

Griffin JH, Zlokovic B, Fernandez JA. Activated protein C: potential therapy for severe sepsis, thrombosis, and stroke. Semin. Hematol 2002;39:197–205. [PubMed: 12124682]

Guo H, Liu D, Gelbard H, Cheng T, Insalaco R, Fernandez JA, Griffin JH, Zlokovic BV. Activated protein C prevents neuronal apoptosis via protease activated receptors 1 and 3. Neuron 2004;41:563–572. [PubMed: 14980205]

Han MH, Hwang SI, Roy DB, Lundgren DH, Price JV, Ousman SS, Fernald GH, Gerlitz B, Robinson WH, Baranzini SE, Grinnell BW, Raine CS, Sobel RA, Han DK, Steinman L. Proteomic analysis of active multiple sclerosis lesions reveals therapeutic targets. Nature 2008;451:1076–1081. [PubMed: 18278032]

Isermann B, Vinnikov IA, Madhusudhan T, Herzog S, Kashif M, Blautzik J, Corat MA, Zeier M, Blessing E, Oh J, Gerlitz B, Berg DT, Grinnell BW, Chavakis T, Esmon CT, Weiler H, Bierhaus A, Nawroth PP. Activated protein C protects against diabetic nephropathy by inhibiting endothelial and podocyte apoptosis. Nat. Med 2007;13:1349–1358. [PubMed: 17982464]

Isobe I, Michikawa M, Yanagisawa K. Enhancement of MTT, a tetrazolium salt, exocytosis by amyloid beta-protein and chloroquine in cultured rat astrocytes. Neurosci. Lett 1999;266:129–132. [PubMed: 10353344]

Jordan J, Galindo MF, Gonzalez-Garcia C, Cena V. Role and regulation of p53 in depolarization-induced neuronal death. Neuroscience 2003;122:707–715. [PubMed: 14622914]

Joyce DE, Gelbert L, Ciaccia A, DeHoff B, Grinnell BW. Gene expression profile of antithrombotic protein c defines new mechanisms modulating inflammation and apoptosis. J. Biol. Chem 2001;276:11199–11203. [PubMed: 11278252]

Kelso EB, Ferrell WR, Lockhart JC, Elias-Jones I, Hembrough T, Dunning L, Gracie JA, McInnes IB. Expression and proinflammatory role of proteinase-activated receptor 2 in rheumatoid synovium: ex vivo studies using a novel proteinase-activated receptor 2 antagonist. Arthritis Rheum 2007;56:765–771. [PubMed: 17328048]

Kerschen EJ, Fernandez JA, Cooley BC, Yang XV, Sood R, Mosnier LO, Castellino FJ, Mackman N, Griffin JH, Weiler H. Endotoxemia and sepsis mortality reduction by non-anticoagulant activated protein C. J. Exp. Med 2007;204:2439–2448. [PubMed: 17893198]

Kim YV, Di Cello F, Hillaire CS, Kim KS. Differential Ca^{2+} signaling by thrombin and protease-activated receptor-1-activating peptide in human brain microvascular endothelial cells. Am. J. Physiol. Cell Physiol 2004;286:C31–C42. [PubMed: 12944324]

Liu D, Cheng T, Guo H, Fernandez JA, Griffin JH, Song X, Zlokovic BV. Tissue plasminogen activator neurovascular toxicity is controlled by activated protein C. Nat. Med 2004;10:1379–1383. [PubMed: 15516929]

Mosnier LO, Griffin JH. Inhibition of staurosporine-induced apoptosis of endothelial cells by activated protein C requires protease-activated receptor-1 and endothelial cell protein C receptor. Biochem. J 2003;373:65–70. [PubMed: 12683950]

Mosnier LO, Gale AJ, Yegneswaran S, Griffin JH. Activated protein C variants with normal cytoprotective but reduced anticoagulant activity. Blood 2004;104:1740–1744. [PubMed: 15178575]

Mosnier LO, Zlokovic BV, Griffin JH. The cytoprotective protein C pathway. Blood 2007;109:3161–3172. [PubMed: 17110453]

Nakanishi-Matsui M, Zheng YW, Sulciner DJ, Weiss EJ, Ludeman MJ, Coughlin SR. PAR3 is a cofactor for PAR4 activation by thrombin. Nature 2000;404:609–613. [PubMed: 10766244]

Neaud V, Duplantier JG, Mazzocco C, Kisiel W, Rosenbaum J. Thrombin up-regulates tissue factor pathway inhibitor-2 synthesis through a cyclooxygenase-2-dependent, epidermal growth factor receptor-independent mechanism. J. Biol. Chem 2004;279:5200–5206. [PubMed: 14623891]

Okamoto S, Li Z, Ju C, Scholzke MN, Mathews E, Cui J, Salvesen GS, Bossy-Wetzel E, Lipton SA. Dominant-interfering forms of MEF2 generated by caspase cleavage contribute to NMDA-induced neuronal apoptosis. Proc. Natl. Acad. Sci. U S A 2002;99:3974–3979. [PubMed: 11904443]

Olianas MC, Dedoni S, Onali P. Proteinase-activated receptors 1 and 2 in rat olfactory system: layer-specific regulation of multiple signaling pathways in the main olfactory bulb and induction of neurite retraction in olfactory sensory neurons. Neuroscience 2007;146:1289–1301. [PubMed: 17434682]

Penninger JM, Kroemer G. Mitochondria, AIF and caspases–rivaling for cell death execution. Nat. Cell Biol 2003;5:97–99. [PubMed: 12563272]

Pompili E, Nori SL, Geloso MC, Guadagni E, Corvino V, Michetti F, Fumagalli L. Trimethyltin-induced differential expression of PAR subtypes in reactive astrocytes of the rat hippocampus. Brain Res. Mol. Brain Res 2004;122:93–98. [PubMed: 14992820]

Riewald M, Ruf W. Protease-activated receptor-1 signaling by activated protein C in cytokine-perturbed endothelial cells is distinct from thrombin signaling. J. Biol. Chem 2005;280:19808–19814. [PubMed: 15769747]

Riewald M, Petrovan RJ, Donner A, Mueller BM, Ruf W. Activation of endothelial cell protease activated receptor 1 by the protein C pathway. Science 2002;296:1880–1882. [PubMed: 12052963]

Romito-DiGiacomo RR, Menegay H, Cicero SA, Herrup K. Effects of Alzheimer's disease on different cortical layers: the role of intrinsic differences in Abeta susceptibility. J. Neurosci 2007;27:8496–8504. [PubMed: 17687027]

Schmidlin F, Amadesi S, Dabbagh K, Lewis DE, Knott P, Bunnett NW, Gater PR, Geppetti P, Bertrand C, Stevens ME. Protease-activated receptor 2 mediates eosinophil infiltration and hyperreactivity in allergic inflammation of the airway. J. Immunol 2002;169:5315–5321. [PubMed: 12391252]

Shibata M, Kumar SR, Amar A, Fernandez JA, Hofman F, Griffin JH, Zlokovic BV. Anti-inflammatory, antithrombotic, and neuroprotective effects of activated protein C in a murine model of focal ischemic stroke. Circulation 2001;103:1799–1805. [PubMed: 11282913]

Song SJ, Pagel CN, Campbell TM, Pike RN, Mackie EJ. The role of protease-activated receptor-1 in bone healing. Am. J. Pathol 2005;166:857–868. [PubMed: 15743797]

Taoka Y, Schlag MG, Hopf R, Redl H. The long-term effects of pre-treatment with activated protein C in a rat model of compression-induced spinal cord injury. Spinal Cord 2000;38:754–761. [PubMed: 11175376]

Tenneti L, Lipton SA. Involvement of activated caspase-3-like proteases in N-methyl-D-aspartate-induced apoptosis in cerebrocortical neurons. J. Neurochem 2000;74:134–142. [PubMed: 10617114]

Thiyagarajan M, Fernandez JA, Lane SM, Griffin JH, Zlokovic BV. Activated protein C promotes neovascularization and neurogenesis in postischemic brain via protease-activated receptor 1. J. Neurosci 2008;28:12788–12797. [PubMed: 19036971]

Uberti D, Belloni M, Grilli M, Spano P, Memo M. Induction of tumour-suppressor phosphoprotein p53 in the apoptosis of cultured rat cerebellar neurones triggered by excitatory amino acids. Eur. J. Neurosci 1998;10:246–254. [PubMed: 9753133]

Uehara A, Muramoto K, Takada H, Sugawara S. Neutrophil serine proteinases activate human nonepithelial cells to produce inflammatory cytokines through protease-activated receptor 2. J. Immunol 2003;170:5690–5696. [PubMed: 12759451]

Wang L, Kittaka M, Sun N, Schreiber SS, Zlokovic BV. Chronic nicotine treatment enhances focal ischemic brain injury and depletes free pool of brain microvascular tissue plasminogen activator in rats. J. Cereb. Blood Flow Metab 1997;17:136–146. [PubMed: 9040492]

Wang H, Yu SW, Koh DW, Lew J, Coombs C, Bowers W, Federoff HJ, Poirier GG, Dawson TM, Dawson VL. Apoptosis-inducing factor substitutes for caspase executioners in NMDA-triggered excitotoxic neuronal death. J. Neurosci 2004;24:10963–10973. [PubMed: 15574746]

Wang Y, Thiyagarajan M, Chow N, Singh I, Guo H, Davis TP, Zlokovic BV. Differential neuroprotection and risk for bleeding from activated protein C with varying degrees of anticoagulant activity. Stroke. 2009in press

Yun LWP, Decarlo AA, Hunter N. Blockade of protease-activated receptors on T cells correlates with altered proteolysis of CD27 by gingipains of *Porphyromonas gingivalis*. Clin. Exp. Immunol 2007;150:217–229. [PubMed: 17937677]

Zhang W, Potrovita I, Tarabin V, Herrmann O, Beer V, Weih F, Schneider A, Schwaninger M. Neuronal activation of NF-kappaB contributes to cell death in cerebral ischemia. J. Cereb. Blood Flow Metab 2005;25:30–40. [PubMed: 15678110]

Zhong, Z.; Hallagan, L.; Chow, N.; Zlokovic, BV. 2006 Neuroscience Meeting Planner. Atlanta, GA: Society for Neuroscience; 2006. Activated protein C inhibits motor neuron degeneration in a transgenic mouse model of amyotrophic lateral sclerosis Program No. 708.8. Online

Zlokovic BV. The blood-brain barrier in health and chronic neurodegenerative disorders. Neuron 2008;57:178–201. [PubMed: 18215617]

Zlokovic BV, Zhang C, Liu D, Fernandez J, Griffin JH, Chopp M. Functional recovery after embolic stroke in rodents by activated protein C. Ann. Neurol 2005;58:474–477. [PubMed: 16130108]

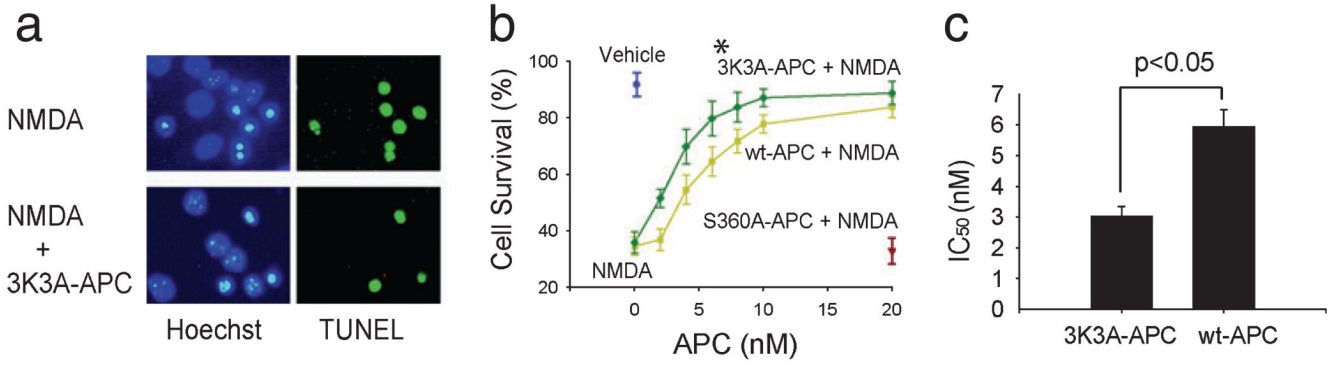

FIG. 1.

Murine recombinant 3K3A-APC blocks NMDA-induced apoptosis in mouse cortical neurons. (a) Immunostaining for terminal deoxynucleotidyl transferase-mediated digoxigenin-dUTP nick-end labeling (TUNEL) and Hoechst at 24:00 h after NMDA in the absence or presence of murine recombinant 3K3A-APC (5 n_M). (b) Dose-dependent neuroprotective effects of murine 3K3A-APC (green) and wt-APC (yellow) at 24:00 h of NMDA (*$P < 0.01$ by two-way ANOVA). Cell survival was quantified with a WST-8 assay. NMDA label at zero concentration APC on the abscissa shows cell survival of neurons treated with NMDA only without 3K3A-APC or wt-APC. Vehicle denotes the basal cell survival rate of neurons in the culture medium in the absence of NMDA. S360A-APC indicates cell survival of neurons treated with NMDA in the presence of enzymatically inactive APC (negative control, brown). (c) IC^{50} (inhibiting concentration) values for 3K3A-APC vs. wt-APC were calculated from experiments shown in (b). All values are mean ± SEM.

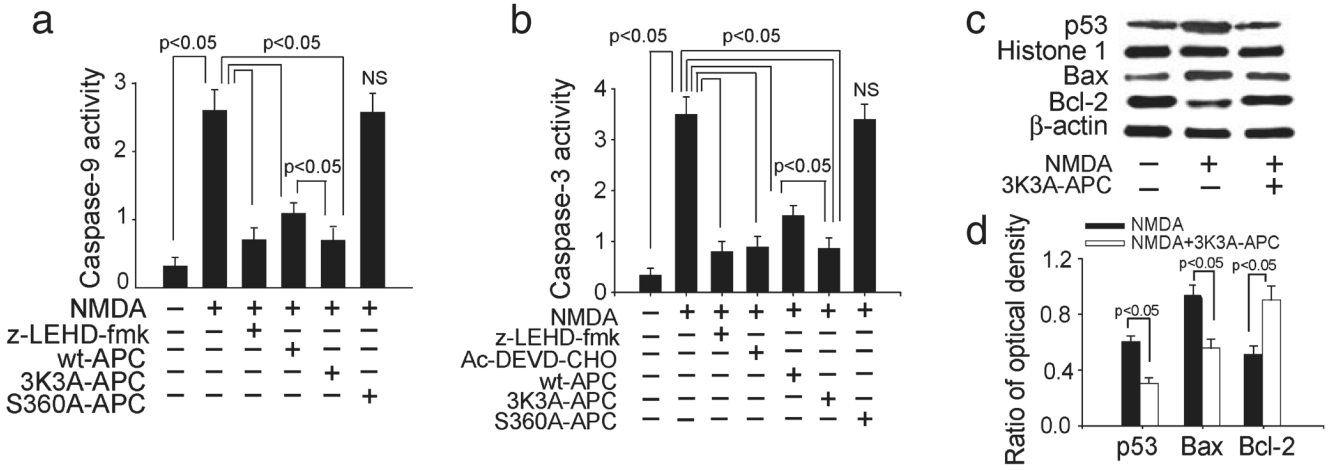

FIG. 2.

Effects of murine recombinant 3K3A-APC on activation of caspases-9 and -3, p53 levels and Bax and Bcl-2 expression in NMDA-treated mouse neurons. Caspase-9 (a) and caspase-3 (b) activities in neurons treated with NMDA in the absence or presence of caspase-9 inhibitor (10 μM; z-LEDH-fmk) and/or caspase-3 inhibitor (50 μM; Ac-DEVD-CHO), murine 3K3A-APC, wt-APC and enzymatically inactive S360A-APC at 5 nM. (c) Western blots for p53 in nuclear extracts, Bax and Bcl-2 in whole-cell extracts from NMDA-treated cells in the absence or presence of murine 3K3A-APC (5 nM). Histone H1 was used as a control for loading of nuclear proteins and β-actin as a control for loading of the whole-cell lysate proteins. (d) Intensity of p53, Bax and Bcl-2 signals measured by scanning densitometry and effects of 3K3A-APC in experiments as in (c). Signal for nuclear p53 was normalized by histone H1 abundance, and signal for Bax and Bcl-2 with β-actin. All values are mean + SEM. NS, non-significant.

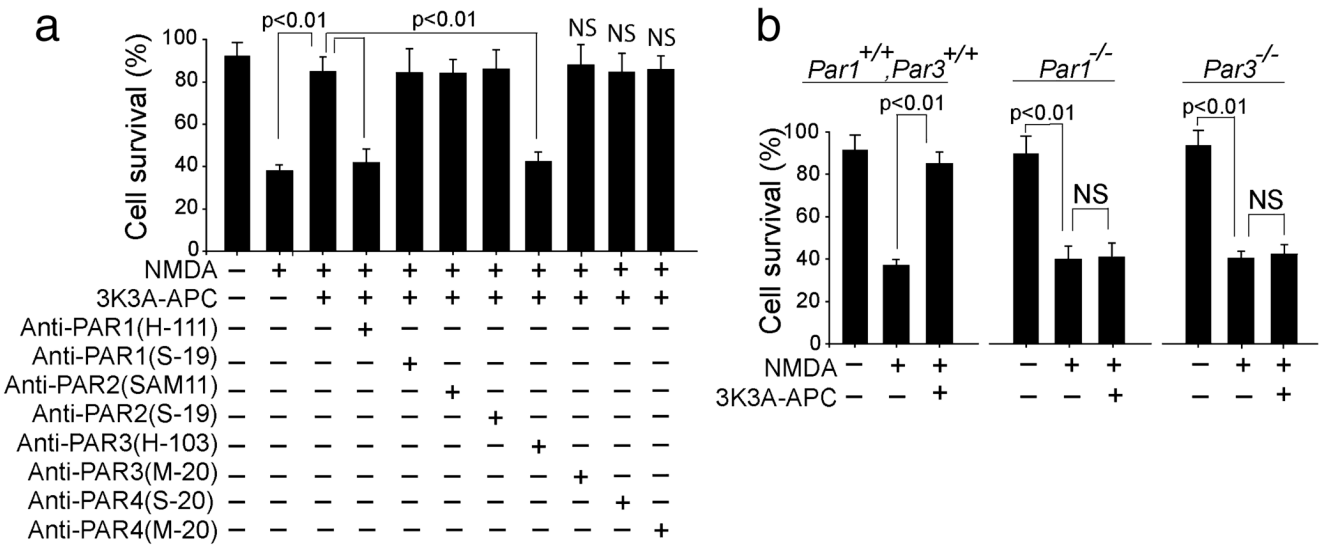

FIG. 3.

The neuroprotection of 3K3A-APC in NMDA-treated neurons is mediated by PAR1 and PAR3. (a) Cortical neurons treated with NMDA and incubated with recombinant murine 3K3A-APC (5 nM and various cleavage-site-blocking antibodies (20 μg/mL) that specifically block the actions of PAR1 (H-111), PAR2 (SAM-11), PAR3 (H-103) and PAR4 (S-20). N-terminal-blocking PAR1 (S-19) and PAR2 (S-19), and C-terminal-blocking PAR3 (M-20) and PAR4 (M-20) antibodies (20 μg/mL) were used as negative controls. Cell survival was quantified with WST-8 assay as in Fig. 1b. (b) Cortical neurons from $PAR1^{-/-}$ and $PAR3^{-/-}$ mice were treated with NMDA and incubated with and without 3K3A-APC (5 nM). Cell survival was quantified with a WST-8 assay. All values are mean + SEM. NS, non-significant.

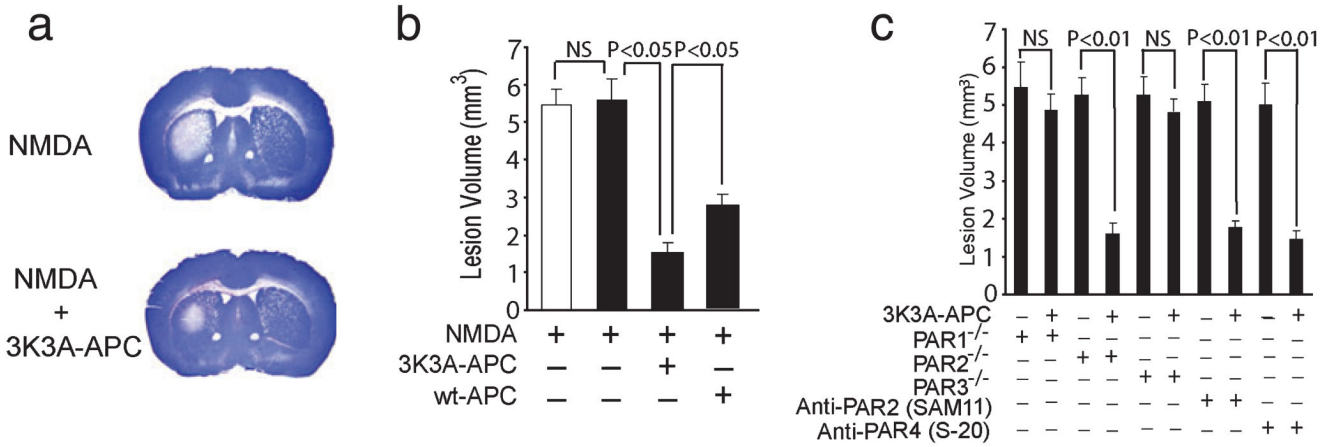

FIG. 4.

Murine 3K3A-APC protects against NMDA-induced lesions *in vivo* via PAR1 and PAR3. (a) Coronal sections of mouse brains at 48:00 h after infusions with NMDA with and without murine 3K3A-APC (0.2 μg). (b) Effects of murine 3K3A-APC (0.2 μg) and wt-APC (0.2 μg) on NMDA lesion volumes at 48:00 h. The white and black bars show the lesion volumes in control C57BL6 mice anesthetized with ketamine and xylazine or isoflurane, respectively. Values are mean + SEM, $n = 5$ mice per group. (c) NMDA-induced lesions in $PAR1^{-/-}$, $PAR2^{-/-}$ and $PAR3^{-/-}$ mice on C57BL6 background infused with vehicle or murine 3K3A-APC (0.2 μg) and in C57BL6 control mice infused with cleavage-site-blocking PAR2 antibody (SAM-11), PAR4 antibody (S-20) and vehicle or 3K3A-APC (0.2 μg). All values are mean + SEM. NS, non-significant.

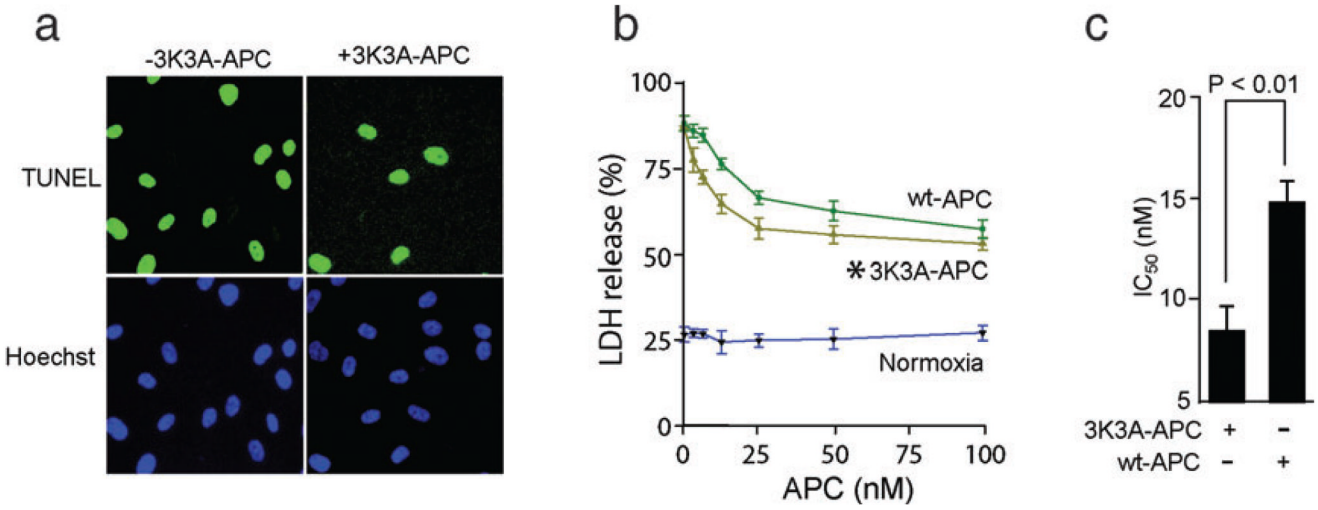

FIG. 5.

Human recombinant 3K3A-APC exerts antiapoptotic activity in hypoxic human BECs. (a) Terminal deoxynucleotidyl transferase-mediated digoxigenin-dUTP nick-end labeling (TUNEL) and Hoechst staining of BECs subjected to OGD for 8:00 h in the absence or presence of human 3K3A-APC (10 nM). (b) Dose-dependent cytoprotective effects of human 3K3A-APC and wt-APC on OGD BECs were quantified with an LDH release assay after 8:00 h of exposure to OGD (*$P < 0.01$ by two-way ANOVA). The basal rate of BEC death under normoxic conditions is also shown. (c) IC_{50} values of 3K3A-APC and wt-APC were calculated from Fig. 1b. All values are mean ± SEM.

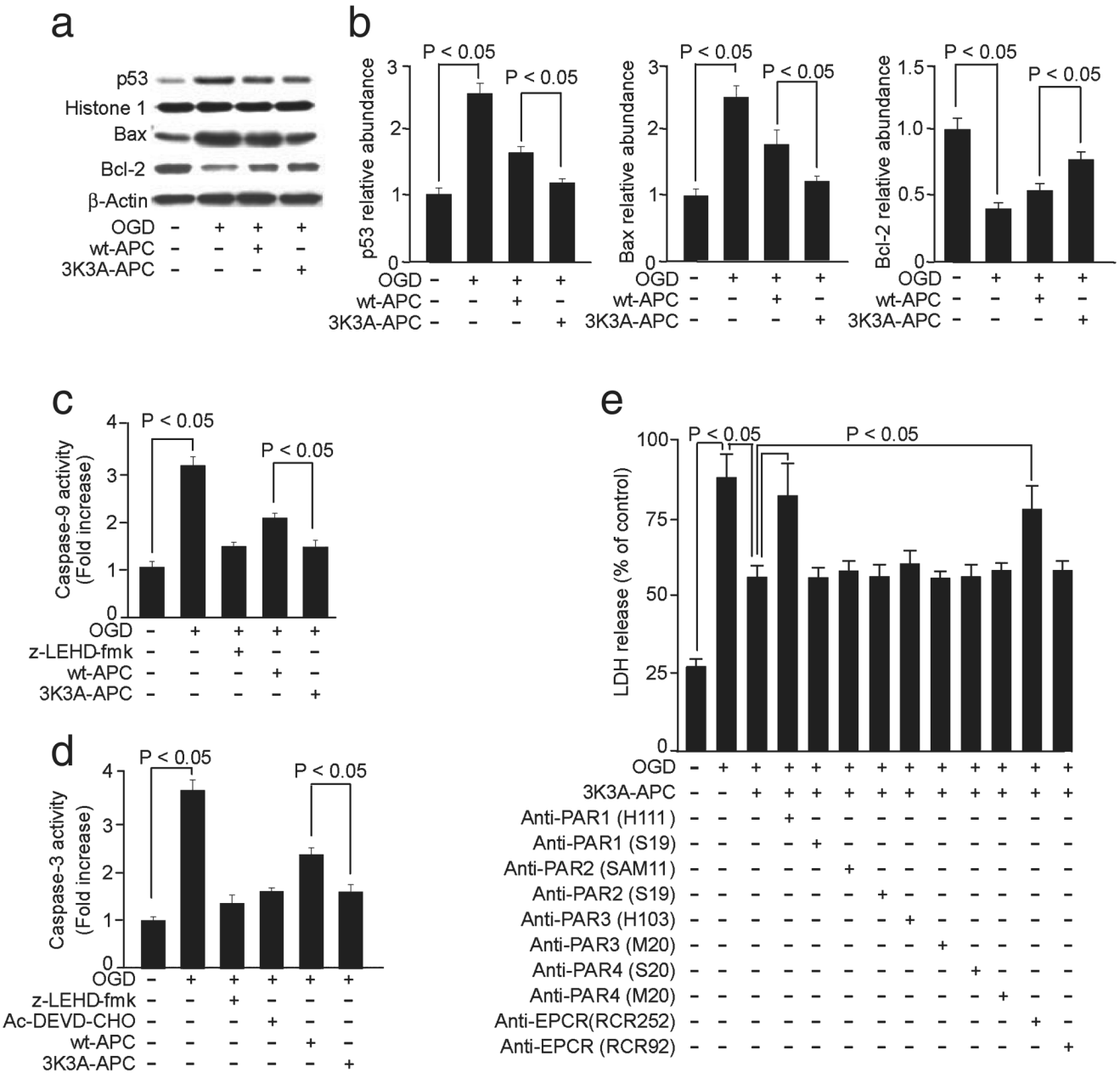

FIG. 6.

Effects of human 3K3A-APC on activation of caspases-9 and -3, p53 levels and Bax and Bcl-2 expression and requirements for EPCR and PAR1 in hypoxic human BECs. (a) Western blots for p53 in nuclear extracts, and Bax and Bcl-2 in whole-cell extracts from BECs treated with OGD for 3:00 h and incubated with and without human 3K3A-APC (10 nM). Histone H1 was used as a control for loading of nuclear p53 protein and β-actin as a control for loading of the whole-cell lysate proteins. (b) Intensity of p53, Bax and Bcl-2 signals measured by scanning densitometry and effects of human 3K3A-APC in experiments as in (a). Signal for nuclear p53 was normalized by histone H1 abundance, and signal for Bax and Bcl-2 with β-actin. Caspase-9 (c) and caspase-3 (d) activities in OGD BECs with and without caspase-9 inhibitor (10 μM; z-LEDH-fmk) and/or caspase-3 inhibitor (50 μM; Ac-DEVD-CHO) and human 3K3A-APC (10

nM). (e) BECs were treated with OGD for 8:00 h and incubated with human 3K3A-APC (10 nM) and various cleavage-site-blocking PAR1 (H-111), PAR2 (SAM-11), PAR3 (H-103) and PAR4 (S-20) antibodies (20 μg/mL) and antibodies against EPCR that either block (RCR252) or do not block (RCR92) APC binding. N-terminal-blocking PAR1 (S-19) and PAR2 (S-19) antibodies and C-terminal-blocking PAR3 (M-20) and PAR4 (M-20) antibodies (20 μg/mL) were used as negative controls. BEC injury was quantified with LDH assay as in Fig. 5b. All values are mean + SEM.

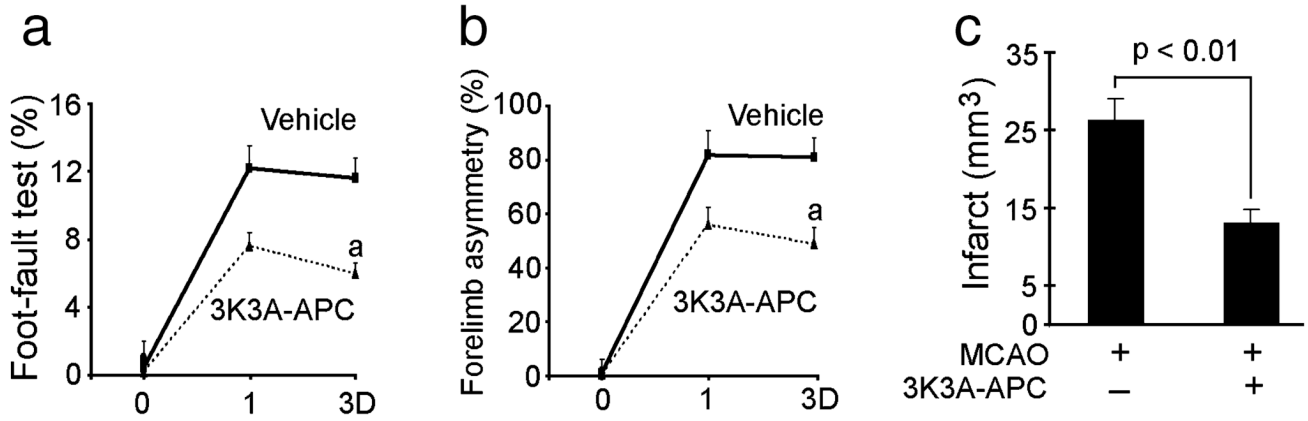

FIG. 7.

Effects of murine recombinant 3K3A-APC on functional recovery and infarct volume after permanent dMCAO. Vehicle or murine 3K3A-APC (0.2 mg/kg) was administered via the tail vein at 4:00 h after permanent dMCAO. Functional tests and infarct volume were determined within 3 days (D) of dMCAO. (a) Foot-fault test. (b) Forelimb asymmetry. (c) Infarct volume. All values are mean + SEM. [a]$P < 0.01$, for 3K3A-APC compared with vehicle by repeated-measures ANOVA.

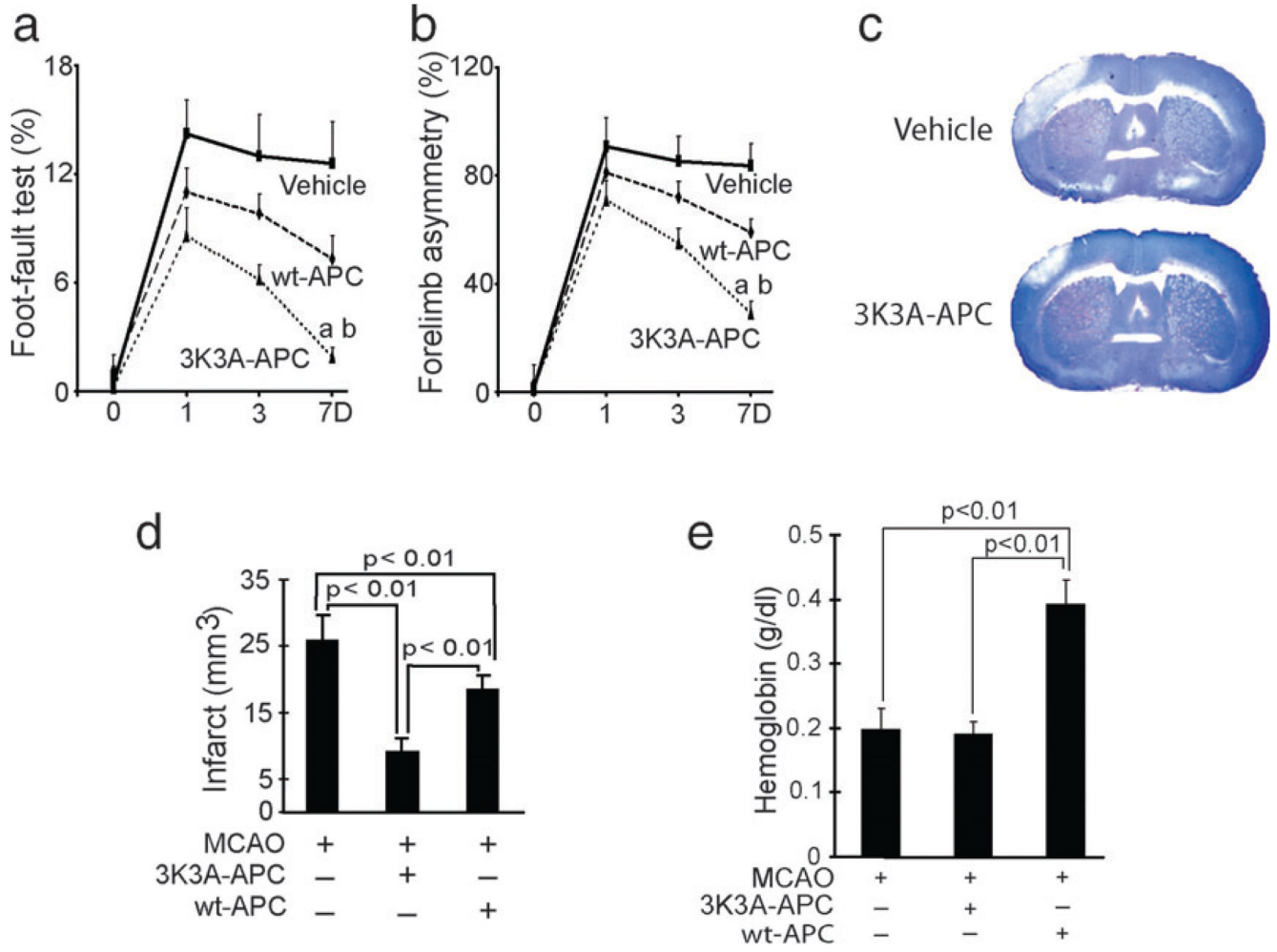

FIG. 8.

Effects of murine recombinant 3K3A-APC and wt-APC on functional recovery and infarct volume after permanent dMCAO. Vehicle, murine wt-APC (0.2 mg/kg) or murine 3K3A-APC (0.2 mg/kg) was administered via the tail vein at multiple times at 12:00 h, 1, 3, 5 and 7 days after permanent dMCAO. Functional tests and infarct volume were determined within 7 days (D) of dMCAO. (a) Foot-fault test. (b) Forelimb asymmetry test. (c) Cresyl violet staining of brain coronal sections of ischemic mice treated with vehicle or 3K3A-APC for 7 days after dMCAO. (d) Infarct volume. (e) Hemoglobin levels in the ischemic hemisphere of mice treated with vehicle, wt-APC or 3K3A-APC for 7 days after dMCAO. All values are mean + SEM. [a]$P < 0.01$, for 3K3A-APC vs. wt-APC; [b]$P < 0.01$, for 3K3A-APC vs. vehicle by repeated-measures ANOVA.